Research Article

SOHAG JOURNAL OF SCIENCES

https://doi.org/10.21608/sjsci.2024.245808.1139

Hybrid Nano Liquid Flow with Electromagnetohydrodynamic and Bioconvective across a Stretching Sheet in a Porous Media with Thermal Buoyancy Effect

M. A. Abdelhafez*, Aboelnour N. Abdalla, Ibrahim A. Abbas, Nourhan M. Elhadidi

Mathematics Department, Faculty of Science, Sohag University, Sohag, Egypt., Sohag University, Sohag 82524, Egypt.
*Email: mostafa.abdallah@yahoo.com

Received: 9th November 2023, **Revised:** 20th December 2023, **Accepted:** 15th January 2024
Published online: 17th January 2024

Abstract: The present study examines the outcome of viscous dissipation chemical reaction, and stratification in porous media on electromagnetohydrodynamic (EMHD) bioconvective hybrid nanofluid flow over an extending surface, using efficient similarity transformations. The system of partial differential equations (PDEs), which is very nonlinear, is converted to a set of ordinary differential equations (ODEs), which is then numerically solved using MATHMATICA's NDSOLVE METHOD and MATLAB's built-in numerical algorithm, bvp4c, is based on finite differences. Graphical representation between the Numerical results for various values of factors related to buoyancy, magnetic, thermal, and solute stratification include profiles of concentration, motion, and temperature. According to the skin friction coefficient, and local Nusselt and Sherwood numbers graphs, the effect of the magnetic field on the velocity profile is shown to be outweighed by the electric field. the electric field dominates the magnetic field in a physical sense. So the velocity profile speeds up with increasing values of M. The fluid temperature and concentration decrease with the increment of the thermal buoyancy λ and solutal stratification parameters, respectively, whereas the magnetic and buoyancy parameters reduce both temperature and concentration profiles. due to the velocity profile acceleration when λ increases.

Keywords: Porous Medium, Shrinking Sheet, Hybrid Nanofluid – Thermal buoyancy.

Nomenclature

u, v	Velocity component(ms^{-1})	s_1	Thermal stratification parameter
T	Temperature of fluid (k)	s_2	Mass stratification parameter
C	Nanoparticles Concentration	s_3	Motile density stratification parameter
N	Microorganism Concentration		**Greek Symbols**
c	Stretching rate (s^{-1})	σ	Electrical conductivity
U_w	Stretching Velocity	ρ	Density (kgm^{-3})
T_w	Surface temperature(k)	θ	Dimensionless temperature
C_w	Surface Concentration of nanoparticles	ψ	Dimensionless Concentration of nanoparticles
N_w	Surface Concentration of microorganism	μ	Dynamic viscosity ($kgm^{-1}s^{-1}$)
T_∞	Ambient temperature(k)	ϑ	Kinematic viscosity (m^2s^{-1})
C_∞	Ambient Concentration of nanoparticles	X	Dimensionless Concentration of Microorganism
N_∞	Ambient Concentration of microorganism	η	Dimensionless variable
T_0	Reference temperature(k)	α	Thermal diffusivity(m^2s^{-1})
C_0	Reference Concentration of nanoparticles	$\emptyset_1$	Volume fraction of CNT
N_0	Reference Concentration of microorganism	$\emptyset_2$	Volume fraction of $F_{e_3}O_4$
E_0	Applied electric field (Vm^{-1})		**Subscripts**
B_0	Magnetic field strength	f	Base fluid
D_B	Brownian diffusion coefficient	nf	Nanofluid
D_m	Microorganisms' diffusion coefficient	hnf	Hybrid Nanofluid
W_c	Maximum cell swimming speed	s_1	CNT nanoparticles
C_P	Specific heat ($J\,Kg^{-1}\,K^{-1}$)	s_2	$F_{e_3}O_4$ nanoparticles
λ	Thermal buoyancy	k	Porous parameter
N_2	Solutal buoyancy parameter	S	Heat generation coefficient

1. Introduction

Nano fluid was used as a coolant in heat transfer equipment is crucial. Additionally, these fluids are crucial for engineering and industry applications such microelectronics, biomedical technology, vehicle cooling and energy production etc, [1, 2]. In order to increase the thermal conductivity. Nanoparticles (size 100 nm) are dispersed into a basic liquid like ethylene, propylene glycol or water. In many industrial and manufacturing processes water and air are examples of classic Newtonian fluids that have been used as cooling fluids, although final product quality inspections tend to indicate that viscous fluids are not the best option. [3] examined a two-dimensional constant flow of a water-based hybrid Nano fluid over an irregularly contracting/expanding permeable surface in porous medium. [4] pointed out that the water-based hybrid Nano liquid shown enhanced Nano fluid temperature and velocity when compared to Nano fluid made from engine oil. [2] using a water-based alumina-magnetite hybrid nanomaterial to study the effects on the magneto hydrodynamic (MHD) flow between two parallel plates. They discovered that the volume proportion of alumina and magnetite nanoparticles caused the heat transfer rate to decrease. [5] observed a rise in the temperature of the Nano liquid for increasing the volume proportion of magnetite and single-wall carbon nanotubes nanoparticles. Additional research on hybrid Nano liquids can be found in [2, 6, 7]. A common process brought on by the erratically moving of microorganisms is bio convection. Applications for bio convective nanomaterial flow in bio microsystems, biotechnology, and biomedicine are extensive. were among the first to study how stable a suspension of microbes and tiny particles was. [8] analysed numerically the effects of temperature and hydrodynamic slip limitations on the water-based bio-nanomaterial containing microorganisms using the Runge-Kutta-Fehlberg and ND Solve (Mathematica) method. They noticed that increasing the bio convection Peclet number tended to increase the quantity of motile microorganisms. Alshomrani investigated the result of repeated slip on bioconvective flow. [9, 10] With the use of the successive local linearization method, it was examined how activation energy affected the suspension of nanoparticles and microbes in a magnetic fluid. Additional research on bioconvective fluxes is available in [11-14]. A process known as stratification begins when there are variations in the profiles of mass, heat, and motile density or when separate fluids are present. Alsaedi looked into the impact of stratification on hydro magnetic mixed convective Nano liquid flow. [15] the homotopy analysis method (HAM) is used. They noticed that increasing the thermal stratification parameter caused the Nano liquid temperature to fall. [16] observed a (CNT) drop in the Nano fluid temperature and volume fraction with regard to thermal and solutal stratification parameters, respectively, while considering the impact of double stratification on carbon nanotube Nano fluid flow. [16] studied the effect of the thermal stratification parameter on the flow of a Nano liquid made of ethylene glycol. Several works that deal with the implications of stratification are discussed in [17,18]. Magnetohydrodynamics (MHD) is a subject of fluid dynamics that studies the effects of magnetic fields on electrically conducting fluids, such as plasma. [19]. Abbas et al. applied the finite difference method to study the effects of temperature variations on living tissues by using bioheat models with experimental study [20, 21].

The research community is increasingly turning to statistical techniques including sensitivity analysis, regression analysis, and response surface methodology. A statistical procedure called response surface methodology (RSM) examines how individualistic variables (factor variables/parameters) affect physical quantities (reliant variables/response). [22] investigated how the heat transfer rate was affected by the Hartmann number, thermal radiation, and thermal slip parameter. using RSM and sensitivity analysis. They concluded that smaller Hartmann number values correspond to the highest heat transmission rate. [21] The current study is being conducted to examine the impacts of stratification over a linearly scale on the bioconvective EMHD hybrid nanomaterial flow a stretched sheet as a result of the aforementioned studies. The current research has applications in the treatment of cancer, the administration of therapeutic drugs, and biomedical imaging [23-25]. The governing model is reduced to a set of ordinary (similarity) differential equations and then, numerically computed using the efficient bvp4c solver in the MATLAB software.

The primary goals of this work are:

1- Analyse the effects of important variables on the flow profiles.
2- Comparatively analyse the hybrid Nano liquid flow employing SWCNT and MWCNT nanoparticles that contain Fe_3o_4..
3- Make an estimation of the interacting impacts of the important factors pertaining to the drag coefficient using a five-level, four-factor RSM methodology.

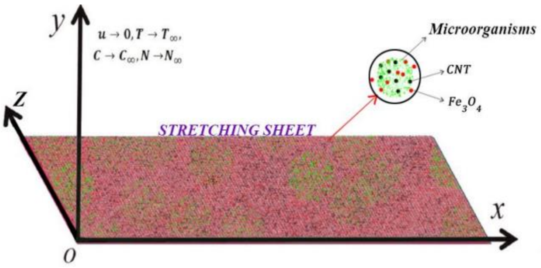

$$\boldsymbol{u_w = cx\,, v = 0, C = C_w, N = N_w\,, T = T_w}$$

Fig1(a): physical model.

2. Mathematical Model

Imagine a two-dimensional bioconvective steady flow past a sheet that is stretched linearly and has a velocity $(U_w(x) = cx)$ positioned on the x-axis, the area is occupied by a Nanofluid of water –based carbon nanotubes that contains microorganisms. E_0, B_0 are delivered perpendicular to the fluid flow, producing the strength of the external electric field(E_0) and a magnetic field outside that is both strong and external (B_0) is $y > 0$. Due on the presumption of an extremely low Reynolds number for magnetism, anything which is induced magnetically was untended. Also included are the effects of stratification, viscosity dissipation, and chemical reactivity. Tiwari – Das nano liquid model usage.[26] The governing equations are represented by:[15, 27-29]

$$u_x + v_y = 0 \tag{1}$$

$$u\frac{\partial u}{\partial x} + v\frac{\partial u}{\partial y} = \left(\frac{\mu_{hnf}}{\rho_{hnf}}\right)\frac{\partial^2 u}{\partial y^2} + \frac{\sigma_{hnf}}{\rho_{hnf}}(E_0B_0 - B_0^2u) - \frac{\vartheta_f}{k_1}u + g(\beta_T(T - T_\infty) + \beta_C(C - C_\infty)) \tag{2}$$

$$u\frac{\partial T}{\partial x} + v\frac{\partial T}{\partial y} = (\alpha_{hnf})\frac{\partial^2 T}{\partial y^2} + \frac{\mu_{hnf}}{(\rho c_p)_{hnf}}\left(\frac{\partial u}{\partial y}\right)^2 + \frac{Q}{(\rho c_p)_{hnf}}(T - T_\infty) \tag{3}$$

$$u\frac{\partial C}{\partial x} + v\frac{\partial C}{\partial y} = (D_B)\frac{\partial^2 C}{\partial y^2} - K_r(C - C_\infty) \tag{4}$$

$$u\frac{\partial N}{\partial x} + v\frac{\partial N}{\partial y} + \frac{bw_C}{(c_w - c_0)}\left(\frac{\partial}{\partial y}\left(N\frac{\partial C}{\partial y}\right)\right) = (D_m)\frac{\partial^2 N}{\partial y^2} \tag{5}$$

Depending on the boundary restriction:

$$u = U_w(x) = cx, v = 0, T = T_w = T_0 + \delta_1 x, \\ C = C_w = C_0 + \varepsilon_1 x, N = N_w = N_0 + \xi_1 x \ \ at\ y=0 \quad (6)$$

$$u \to 0, T = T_\infty = T_0 + \delta_2 x, C \to C_\infty = C_0 + \\ \varepsilon_2 x, N \to N_\infty = N_0 + \xi_2 x \ \text{ as y} \to \infty \quad (7)$$

In order to solve the current issue, hybrid nanofluid models are (see[30-32])

Viscosity dynamic effect:

$$\frac{\mu_{hnf}}{\mu_f} = \frac{1}{(1-\emptyset_1)^{2.5}(1-\emptyset_2)^{2.5}} = \frac{1}{A_1}$$

Density effect:

$$\frac{\rho_{hnf}}{\rho_f} = (1-\emptyset_2)\left[1-\emptyset_1+\emptyset_1\left(\frac{\rho_{s1}}{\rho_f}\right)\right] + \emptyset_2\left(\frac{\rho_{s2}}{\rho_f}\right) = A_2$$

Specific heat effect:

$$\frac{(\rho c_p)_{hnf}}{(\rho c_p)_f} = (1-\emptyset_2)\left[1-\emptyset_1+\emptyset_1\left(\frac{\rho c_{p_{s1}}}{\rho c_{p_f}}\right)\right] + \emptyset_2\left(\frac{\rho c_{p_{s2}}}{\rho c_{p_f}}\right) = A_3$$

Thermal conductivity effect:

$$\frac{k_{hnf}}{k_f} = A_4,$$

where

$$\frac{k_{hnf}}{k_{nf}} = \frac{1-\emptyset_2+2\emptyset_2\left(\frac{k_{s2}}{k_{s2}-k_{nf}}\right)\ln\left(\frac{k_{s2}+k_{nf}}{2k_{nf}}\right)}{1-\emptyset_2+2\emptyset_2\left(\frac{k_{nf}}{k_{s2}-k_{nf}}\right)\ln\left(\frac{k_{s2}+k_{nf}}{2k_{nf}}\right)},$$

$$\frac{k_{nf}}{k_f} = \frac{k_{s1}+2k_f-2\emptyset_1\,(k_f-k_{s1})}{k_{s1}+2k_f-\emptyset_1\,(k_f-k_{s1})}$$

Electrical conductivity effect:

$$\frac{\sigma_{hnf}}{\sigma_f} = 1 + \frac{3\left(\frac{\emptyset_1\sigma_1-\emptyset_2\sigma_2}{\sigma_f}-(\emptyset_1+\emptyset_2)\right)}{2+\left(\frac{\emptyset_1\sigma_1-\emptyset_2\sigma_2}{(\emptyset_1+\emptyset_2)\sigma_f}\right)-\left(\frac{\emptyset_1\sigma_1-\emptyset_2\sigma_2}{\sigma_f}-(\emptyset_1+\emptyset_2)\right)} = A_5$$

Similarity transformations take as follow:[15, 27]

$$u = cxf'(\eta), v = -\sqrt{c\vartheta_f}f(\eta), \eta = \sqrt{\frac{c}{\vartheta_f}}\,y, \\ \theta(\eta) = \frac{(T-T_\infty)}{(T_W-T_0)}, \psi(\eta) = \frac{(C-c_\infty)}{(c_w-c_0)}, \\ X(\eta) = \frac{N-N_\infty}{N_w-N_0} \quad (8)$$

The regulating formulas and the boundary circumstances change when these comparable factors and the hybrid nanofluid constants are given as:

$$f''' + A_1A_2ff'' - (A_1A_2F' + A_1A_5M)F' + \\ A_1A_5ME - A_1A_2Kf' + A_1A_2\lambda\theta + A_1A_2N_2\psi = 0 \quad (9)$$

$$A_4\theta'' + A_3p_rf\theta' + \frac{p_r}{A_1}E_cf''^2 + Sp_r\theta = 0 \quad (10)$$

$$\psi'' + l_ef\psi' - k_rl_e\psi = 0 \quad (11)$$

$$X'' + (l_bf - p_e\psi')X' - p_eX\psi''\Omega p_e\psi'' = 0 \quad (12)$$

Currently, initial conditions and boundary conditions can be described by:

$$f(0) = 0 \ \ , f'(0) = 1\,, \theta(0) = 1 - S_1 \ \ , \psi(0) \\ = 1 - S_2\,, X(0) = 1 - S_3 \quad (13)$$

$$f'(\infty) \to 0, \quad \theta(\infty) = 0\,, \quad \psi(\infty) \to 0\,, \\ X(\infty) \to 0 \ as\ \eta \to \infty \quad (14)$$

Such that M (Hartmann number) $= \frac{\sigma_f}{c\rho_f}B_0^2$,E(electric field parameter) $= \frac{E_0}{B_0U_w}$, p_r (Prandtl number) $= \frac{\vartheta_f}{\alpha_f}$, K(Porous parameter) $= \frac{\vartheta_f}{ck_1}$, λ (Thermal buoyancy) $=\frac{G_r}{Re^2}$, N_2(Solutal buoyancy parameter) $= \frac{G_r^*}{Re^2}$,S (Heat generation coefficient) $= \frac{Q}{c(\rho c_p)_f}$,Kr (chemical reaction parameter) $= \frac{K_r}{c}$, E_c (Eckert number) $= \frac{(cx)^2}{(c_p)_f(T_W-T_0)}$, l_e (Lewis number)$=\frac{\vartheta_f}{D_B}$, l_b (bioconvection, Lewis number)$=\frac{\vartheta_f}{D_m}$, p_e (bioconvection Peclet number)$=\frac{bw_C}{D_m}$,and Ω(microorganism concentration difference parameter)$=\frac{N_\infty}{(N_w-N_0)}$ are the dimensionless quantities.

Physical quantities:

include the local Sherwood number, skin friction coefficients, local motile density number and local Nusselt number, which measure the mass transfer rate, surface drag, heat transfer rate and microbe density number, respectively [33, 34].

skin friction coefficients,

$$Cf_x = \frac{\mu_{hnf}\left(\frac{\partial u}{\partial y}\right)_{y=0}}{\rho_f(U_w)^2} \Longrightarrow Re_x^{\frac{1}{2}}Cf_x = \frac{f''(0)}{A_1} \quad (15)$$

Nusselt number,

$$Nu_x = -\frac{xK_{hnf}\left(\frac{\partial T}{\partial y}\right)_{y=0}}{K_f(T_w-T_0)} \Longrightarrow Re_x^{-\frac{1}{2}}Nu_x \\ = -A_4\theta'(0) \quad (16)$$

Sherwood number,

$$Sh_x = -\frac{xD_B\left(\frac{\partial C}{\partial y}\right)_{y=0}}{D_B(C_w-C_0)} \Longrightarrow Re_x^{-\frac{1}{2}}Sh_x = -\psi'(0) \quad (17)$$

Microorganism density number,

$$Nn_x = -\frac{xD_m\left(\frac{\partial N}{\partial y}\right)_{y=0}}{D_m(N_w-N_0)} \Longrightarrow Re_x^{-\frac{1}{2}}Nn_x = -X'(0) \quad (18)$$

where $Re_x = \frac{U_w x}{\vartheta_f}$.

3. Numerical Procedure and Validation:

Since equations (9) to (12) are greatly nonlinear, it is very hard to find a closed-form or an exact solution. Hence an approximate solution is computed numerically by employing the bvp4c algorithm (a finite difference based built-in numerical procedure) in MATLAB. To this purpose, let

$$f = z_1,\ f' = z_2, f'' = z_3,\ f''' = z_3',\ \theta = z_4, \theta' = z_5, \theta'' = z_5',\ \psi = z_6\ , \psi' = z_7, \psi'' = z_7', X = z_8, X' = z_9, X'' = z_9'.$$

The transmuted system of first-order ODEs are given as:

$$z_1' = z_2$$
$$z_2' = z_3$$
$$z_3' = -\mathrm{A_1A_2z_1z_3} + (\mathrm{A_1A_2z_2} + \mathrm{A_1A_5M})\mathrm{z_2} - \mathrm{A_1A_5ME} + \mathrm{A_1A_2Kz_2} - \mathrm{A_1A_2\lambda z_4} - \mathrm{A_1A_2N_2z_6}$$
$$z_4' = z_5$$
$$z_5' = -\frac{A_1A_3p_rz_1z_5 + A_1p_rE_cz_3^2\ + A_1Sp_rz_4}{A_4A_1}$$
$$z_6' = z_7$$
$$z_7' = -l_ez_1z_7 + l_ez_6$$
$$z_9' = (z_8{+}\Omega)z_7' {-} (l_bz_1 - p_ez_7)z_9$$

with

$$z_1(0) = 0, z_2(0) = 1, z_4(0) = 1 - S_1, z_6(0) = 1 - S_2, z_8(0) = 1 - S_3$$
$$z_2(\infty) = 0, z_4(\infty) = 0, z_6(\infty) = 0, z_8(\infty) = 0$$

The bvp4c algorithm uses a three-stage Lobatto IIIa formula built on an association polynomial that returns a -continuous solution which is uniformly accurate to the fourth- $C1$ order. The veracity of the code and the validation of the current problem have been adjudged through a restrictive comparison with the already published work of Khan & Pop [44] (see Table 1).

Table1: Thermophysical properties (see [30, 35, 36])

Physical properties	K	σ	ρ	c_p
Pure water	0.613	0.05	997.1	4179
SWCNT	6600	10^6	2600	425
MWCNT	3000	10^7	1600	796
Fe_3o_4	9.7	25000	5180	670

Table 2: Comparison of $Re_x^{-\frac{1}{2}}Nu_x$ for differing p_r values when $M = E = k_r = E_c = l_b = l_e = p_e = \Omega = \lambda = S = K = N_2 = S_1 = S_2 = S_3 = 0$

p_r	$Re_x^{-\frac{1}{2}}Nu_x$	
	[37]	Current study
0.7	0.4539	0.4540
2	0.9113	0.91273
7	1.8954	1.934
20	3.3539	3.3538
70	6.4621	6.4755

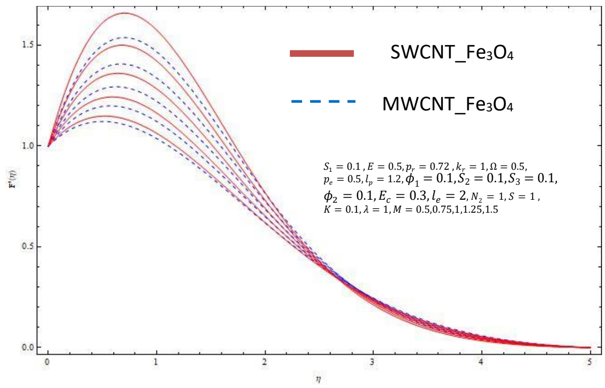

Fig1(b):variation in $f'(\eta)$ with M

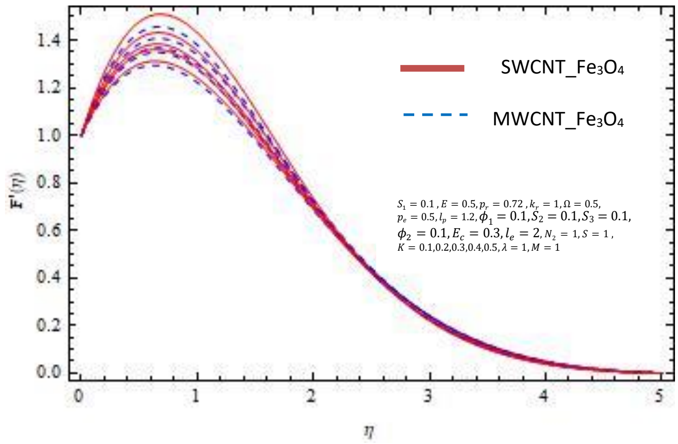

Fig 2: variation in $f'(\eta)$ with K

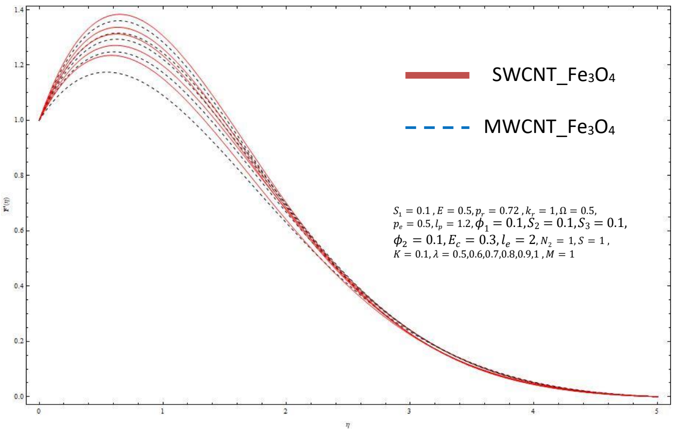

Fig 3: variation in $f'(\eta)$ with λ

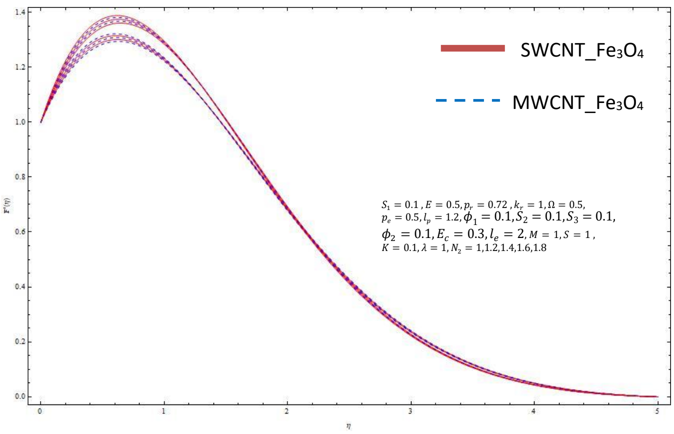

Fig 4: variation in $f'(\eta)$ with N_2

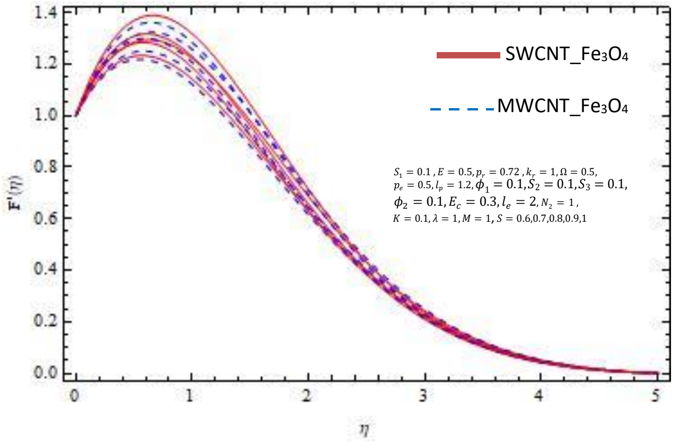

Fig 5: variation in $f'(\eta)$ with S

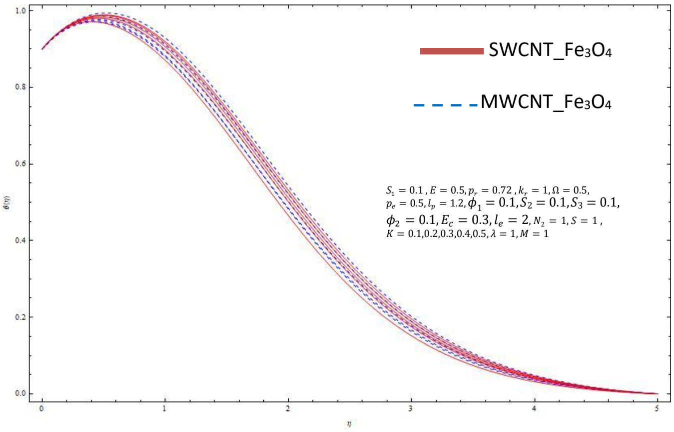

Fig 6: variation in $\theta(\eta)$ with K

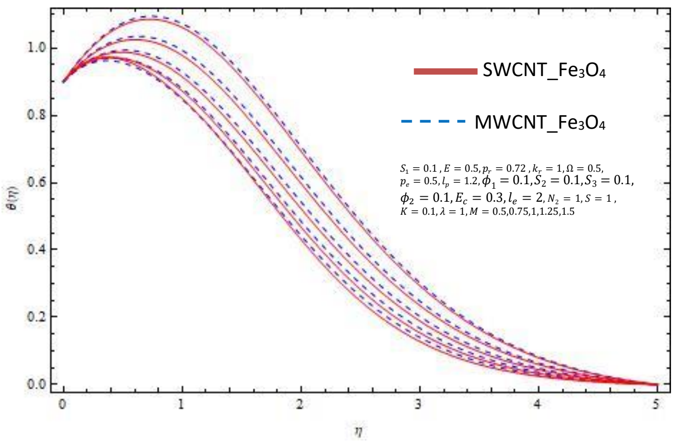

Fig 7: variation in $\theta(\eta)$ with M

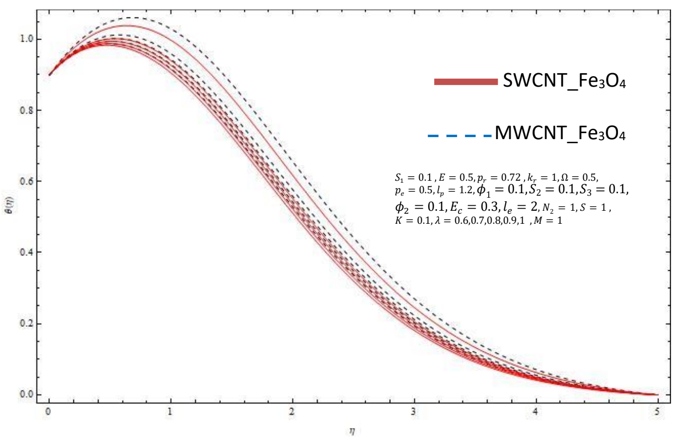

Fig 8: variation in $\theta(\eta)$ with λ

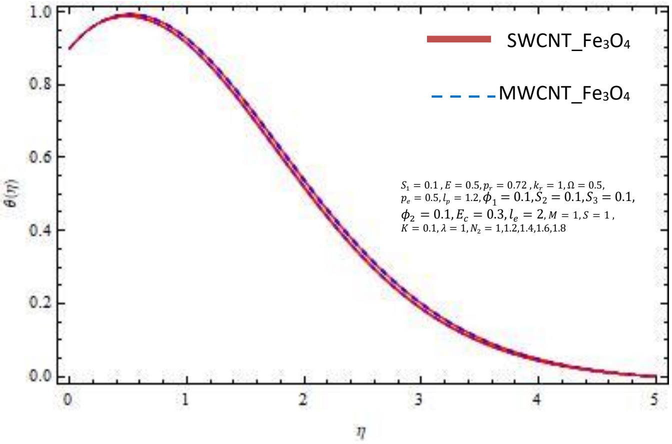

Fig 9: variation in $\theta(\eta)$ with N_2

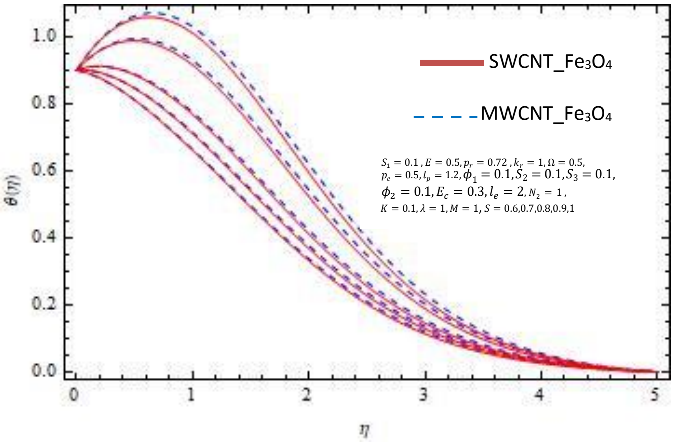

Fig 10: variation in $\theta(\eta)$ with **S**

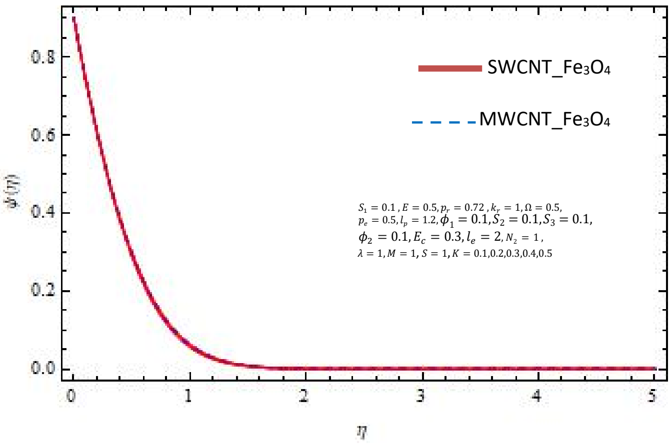

Fig 11: variation in $\psi(\eta)$ with K

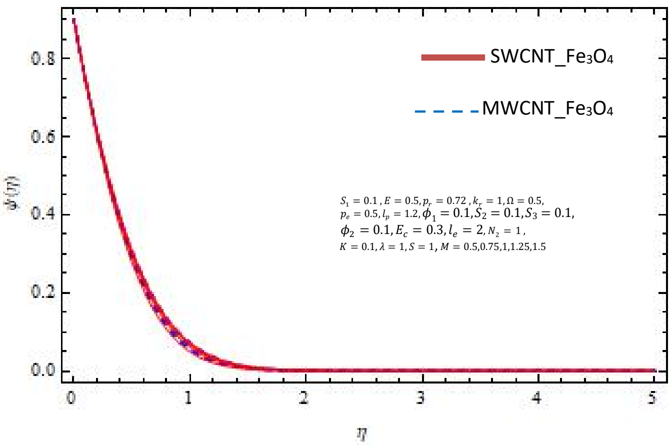

Fig 12: variation in $\psi(\eta)$ with M

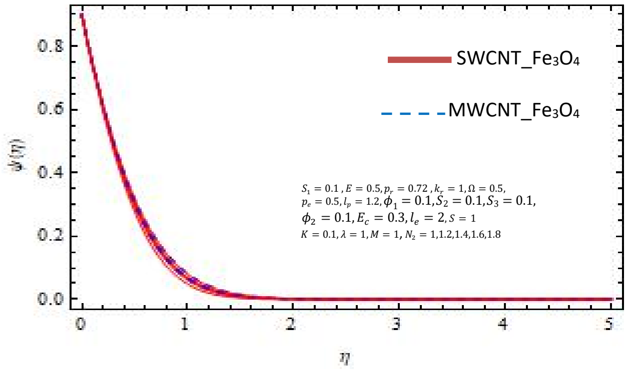

Fig 13: variation in$\psi(\eta)$with N_2

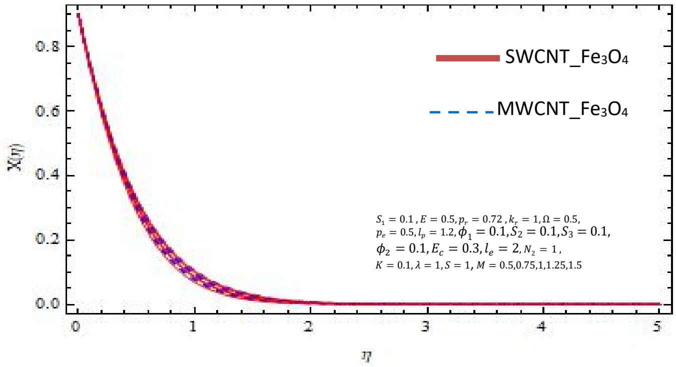

Fig 17: variation in $X(\eta)$with M

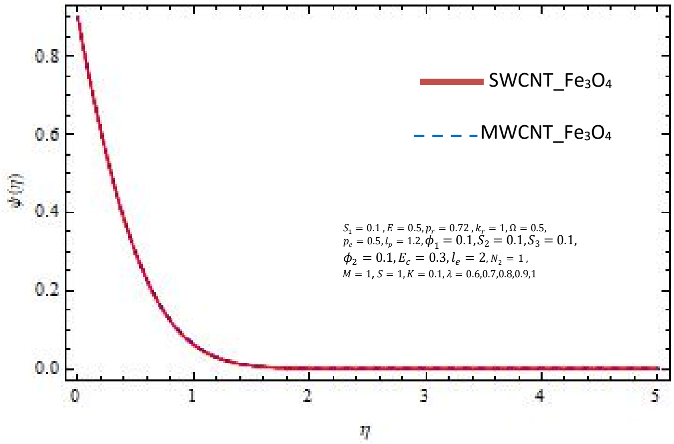

Fig 14: variation in $\psi(\eta)$with λ

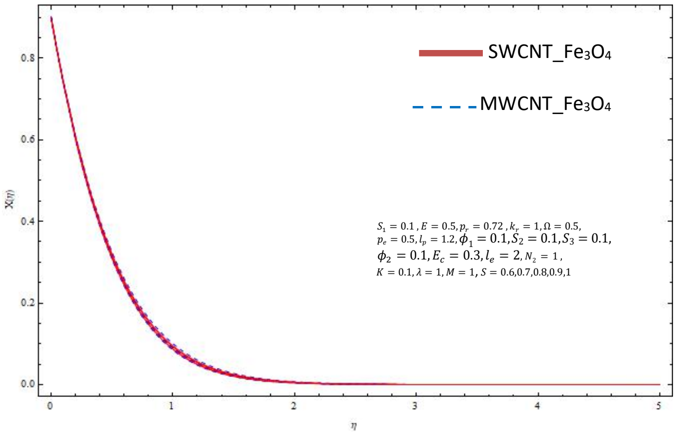

Fig 18: variation in$X(\eta)$with S

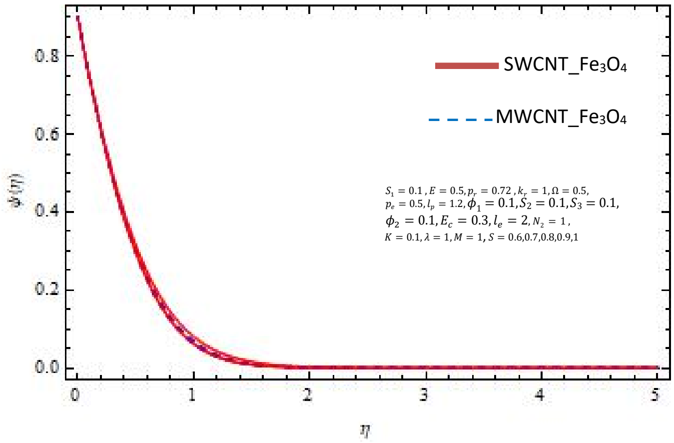

Fig 15: variation in $\psi(\eta)$with S

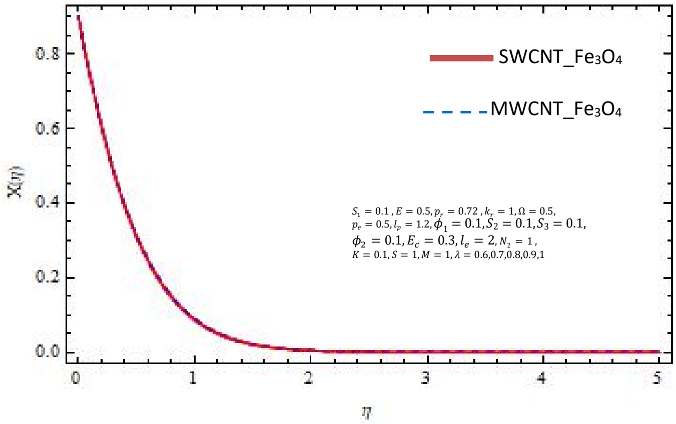

Fig 19: variation in $X(\eta)$with λ

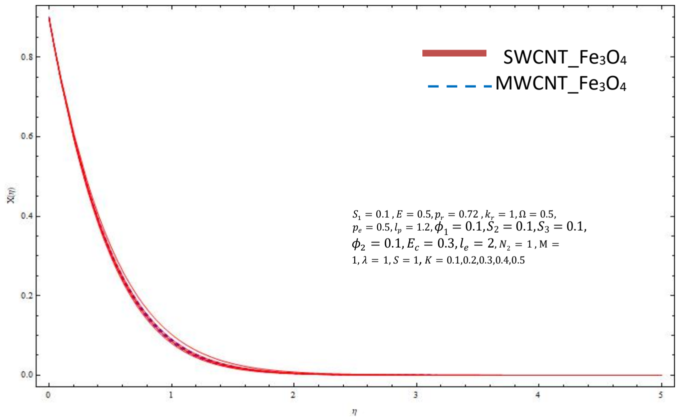

Fig 16: variation in $X(\eta)$with K

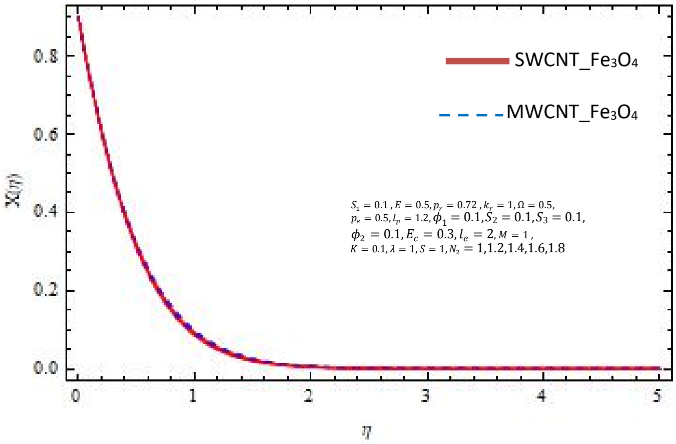

Fig 20: variation in $X(\eta)$with $\boldsymbol{N_2}$

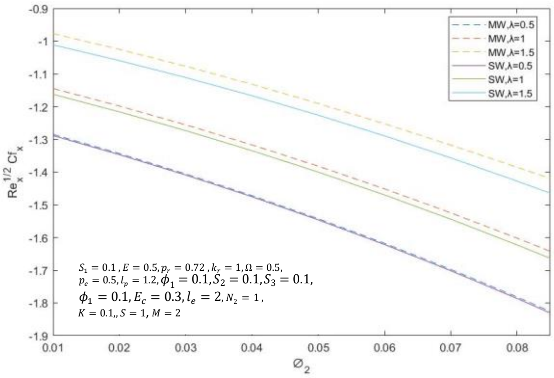

Fig21: variation of $Re_x^{\frac{1}{2}}\,Cf_x$with λ

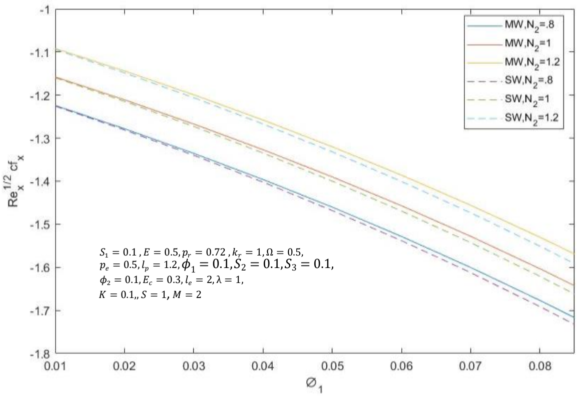

Fig22: variation of $Re_x^{\frac{1}{2}}\,Cf_x$with N_2

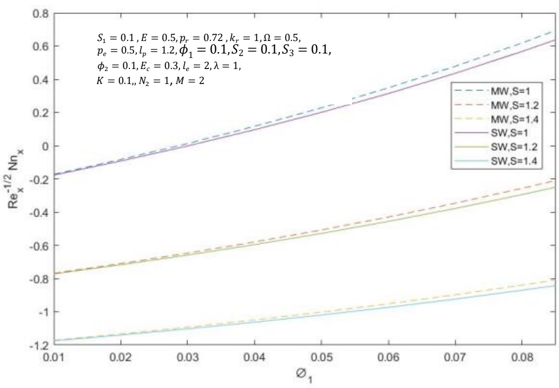

Fig23: variation of $Re_x^{-\frac{1}{2}}\,Nn_x$with S

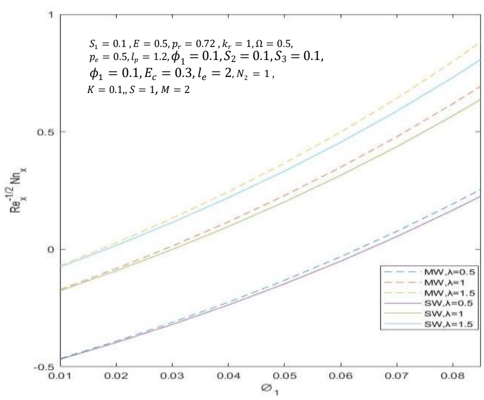

Fig24: variation of $Re_x^{-\frac{1}{2}}\,Nn_x$with λ

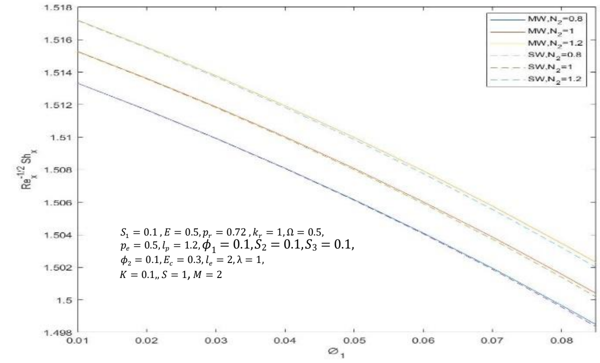

Fig25: variation of $Re_x^{-\frac{1}{2}}\,Sh_x$with N_2

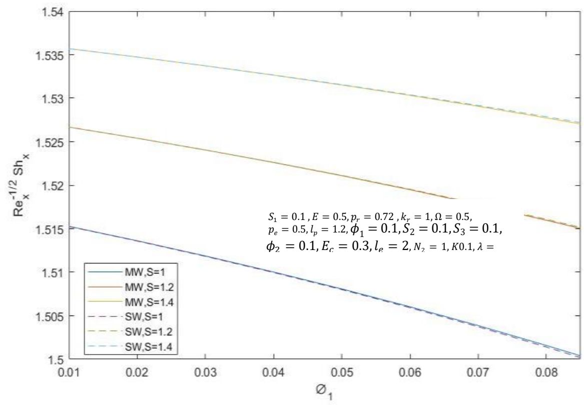

Fig26: variation of $Re_x^{-\frac{1}{2}}\,Sh_x$with S

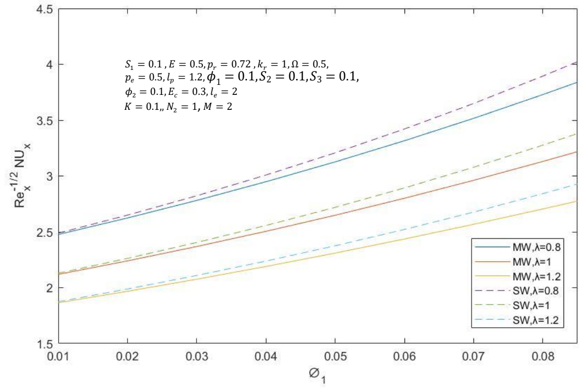

Fig27: variation of $Re_x^{-\frac{1}{2}}\,Nu_x$with λ

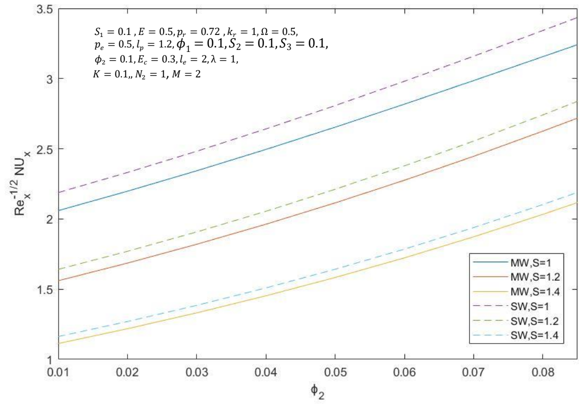

Fig28: variation of $Re_x^{-\frac{1}{2}}\,Nu_x$with S

4. Discussion:

The set of ordinary differential equations that are nonlinear (9)-(12) according to the boundary restrictions (13,14) MATLAB's bvp4c function is used to solve numerically and NDsolve inside MATHMATICA The pre- organized data for a finite-difference function is the built-in bvp4c function. algorithm called Lobatto IIIa a formula in three steps using fourth-order precision. The outcomes demonstrate how the thermal buoyancy parameter λ has an impact, porous factor K, the heat generation coefficient S, the solutal buoyancy parameter N_2 , thermal stratification s_1 as well as zonal stratification s_2 characteristics related to the concentration, temperature, velocity profiles, the skin friction coefficient and the local Nusselt as well as Sherwood numerals. The stretching/shrinking sheet in a porous media saturated with a viscous fluid is represented by K ≠0 for the porous parameter.

Figs.**1(b)-20** show the effects of different physical quantities' characteristics, microbial concentration profile $(X(\eta))$, temperature profile of the nanofluid $(\theta(\eta))$, velocity profile $\left(f'(\eta)\right)$,and nanofluid concentration profile $\left(\psi(\eta)\right)$ are all taken into consideration regarding $SWCNT - Fe_3o_4$. and $MWCNT - Fe_3o_4$. hybrid nanofluids.

The Prandtl number, the Lewis numbers, the Lewis numbers for bioconvection, and Infinity are all set at 0.72,2 ,1.2, and 5 correspondingly. Table **2** also lists the fluid used as the base and the nanoparticles thermophysical characteristics. For example, result of colliding with the fluid motion and reducing velocity, the resistive force created when a magnetic field function is present, the Lorentz force be a resistive force. In Fig. **1(b)** the velocity profile speeds up with increasing values of M This is because the electric field dominates the magnetic field in a physical sense. Fig. **3** The buoyancy effect, λ, causes the fluid rate to accelerate. Convective transport thus takes over and becomes more fluid as it enters the wake zone. As same Figs. **2, 4, 5** show that velocity profile speeds up at different values of K, S, N_2. Fig. **6** demonstrate how the fluid's temperature decreases as thermal buoyancy λ increases. It is observed that the thermal resistance created through the fluid particles' impact causes the temperature that of nanoliquids to increase.

Figs. **7-10** show how $(\theta(\eta))$ improves with increasing values of K, S, N_2, M , correspondingly. On a physical level, it is related to the enhancement of the nanofluid's heat conductivity that occurs as a result of the greater occupancy of nanoparticles Additionally, A greater temperature of the nanofluid is seen regarding liquid-based hybrid SWCNT–Fe_3o_4. Fig**14,15** show the effects of the heat and spatial factors of stratification on the concentration profile, respectively. The concentration's initial and secondary solutions profile decrease upon improving the stratification parameters, but it's crucial to regulate the thermal stratification parameter's value S. Fig**11-13** Applying thermal buoyancy causes a drop in fluid concentration., the heat generation coefficient S and the solutal buoyancy parameterN_2 and magnetic parameters M.

The thickness of concertation eventually decreases as the thermal conductivity of nanofluid increases and permeates deeper into the nanoparticles. border stratum. Therefore, a decrease in concentration characteristics correlates to an increase in the thermophoresis parameter.

Fig. **16-20** illustrates the decreasing nature of $\chi(\eta)$ with Hartmann number M, the thermal buoyancy parameter λ, porous parameter K, The coefficient of heat generation S and the solutal buoyancy parameterN_2 values. Figs. **21-28** Show how the thermal buoyancy parameter λ is affected by the skin friction coefficient, local Nusselt, microorganism density number, and Sherwood numbers using specific values of S and N_2.The simultaneous effects of efficient factors affecting the rate of heat transfer and surface drag are explored in Figs. **21** through **28**. Figs. **21,22,25** and **26** show that the drag coefficient increases and decreases with N_2, λ, S . Additionally, it is noted the heat transmission rate decreases and increasing for principles N_2, λ, S, K see Figs. **23 ,24 ,27**and **28**. The water-based SWCNT $Fe3O4$ hybrid nanofluid is also found to have the lowest surface drag and the fastest rate of heat transfer.

CRediT authorship contribution statement:

Conceptualization, M.A. Abdelhafez and Nourhan M. Elhadidi; methodology, M.A. Abdelhafez; software, Nourhan M. Elhadidi; validation, A.N. Abdalla, I. Abbas and M.A. Abdelhafez; formal analysis, A.N. Abdalla; investigation, M.A. Abdelhafez; resources, Nourhan M. Elhadidi; data curation, Nourhan M. Elhadidi; writing — original draft preparation, Nourhan M. Elhadidi; writing — review and editing A.N. Abdalla and I. Abbas; visualization, M.A. Abdelhafez; supervision, A.N. Abdalla, I. Abbas and M.A. Abdelhafez; project administration, A.N. Abdalla, I. Abbas and M.A. Abdelhafez; funding acquisition, Nourhan M. Elhadidi. All authors have read and agreed to the published version of the manuscript.

Data availability statement

The data used to support the findings of this study are available from the corresponding author upon request.

Declaration of competing interest

The authors declare that they have no known competing financial interests or personal relationships that could have appeared to influence the work reported in this paper.

References

[1] S.U. Choi, and J.A. Eastman, Argonne National Lab. (ANL), Argonne, IL (United States). (1995)
[2] L. J. Abu-Raddad, H. Chemaitelly, H. H. Ayoub, Z. Al Kanaani, A. Al Khal, E. Al Kuwari., Scientific reports, 11 (2021) 6233.
[3] N. Safwa Khashi'ie, N. Md Arifin, E. H. Hafidzuddin and N. Wahi., Applied Sciences, 9 (2019) 2124.
[4] R. Ali, M.I. Asjad, and A. Akgül, Journal of Computational and Applied Mathematics, 383 (2021) 113096.
[5] S. Areekara, F. Mabood, A. Sabu, A. Mathew and I. Badruddin., International Communications in Heat and Mass Transfer, 126 (2021) 105484.
[6] K. Muhammad, T. Hayat, and A. Alsaedi, Waves in Random and Complex Media, (2021) 1-21.
[7] F. Mebarek-Oudina, R. Fares, A. Aissa, R. Lewis and N. Abu Hamdeh., International Communications in Heat and Mass Transfer, 125 (2021) 105279.
[8] Y. Liu, Y. Jian, and W. Tan, International Journal of Heat and Mass Transfer, 127 (2018) 901-913.
[9] A.S. Alshomrani, M.Z. Ullah, and D. Baleanu, Case Studies in Thermal Engineering, 22 (2020) 100798.
[10] M. M. Bhatti, A. Shahid, T. Abbas, S. Z. Alamri and R. Ellahi., Processes, 8 (2020) 328.

[11] Usman, M. Ijaz Khan, S. Ullah Khan, A. Ghaffari, Y.-M. Chu and S. Farooq, International Journal of Modern Physics B, 35 (2021) 2150095.
[12] H. Waqas, M. Hussain, M. Alqarni, M. R. Eid and T. Muhammad, Waves in Random and Complex Media, (2021) 1-18.
[13] H. Waqas, U. Manzoor, M. Alqarni and T. Muhammad., Waves in Random and Complex Media, (2021) 1-16.
[14] N. S. Khashi'ie, N. M. Arifin, I. Pop and R. Nazar., Chinese Journal of Physics, 72 (2021) 461-474.
[15] A. Alsaedi, M. I. Khan, M. Farooq, N. Gull and T. Hayat., Advanced Powder Technology, 28 (2017) 288-298.
[16] M. Ramzan, S. Riasat, Z. Shah, P. Kumam and P. Thounthong., Alexandria Engineering Journal, 59 (2020) 1557-1566.
[17] R. Naz, S. Tariq, and H. Alsulami, Alexandria Engineering Journal, 59 (2020) 247-261.
[18] M. I. Khan, M. Waqas, T. Hayat, M. I. Khan and A. Alsaedi , International Journal of Mechanical Sciences, 131 (2017) 426-434.
[19] I. Ullah, W. A. Khan, W. Jamshed, A. Abd-Elmonem, N. S. E. Abdalla, R. W. Ibrahim., Journal of Molecular Liquids, 392 (2023) 123503.
[20] I. Abbas, A. Abdalla, F. Anwar and H. Sapoor., Sohag Journal of Sciences, 7 (2022) 131-141.
[21] I. Abbas, A. Abdalla, F. Anwar and H. Sapoor., Waves in Random and Complex Media, (2022) 1-15.
[22] A. Mathew, S. Areekara, and A. Sabu, Thermal Science and Engineering Progress, 25 (2021) 101038.
[23] A. Masotti and A. Caporali, International journal of molecular sciences, 14 (2013) 24619-24642.
[24] A. A. Bhirde, V. Patel, J. Gavard, G. Zhang, A. A. Sousa, A. Masedunskas., ACS nano, 3 (2009) 307-316.
[25] X. Fan, G. Jiao, L. Gao, P. Jin and X. Li., Journal of Materials Chemistry B, 1 (2013) 2658-2664.
[26] R.K. Tiwari and M.K. Das, International Journal of heat and Mass transfer, 50 (2007) 2002-2018.
[27] M. Bilal, Alexandria Engineering Journal, 59 (2020) 965-976.
[28] Y. S. Daniel, Z. A. Aziz, Z. Ismail and A. Bahar ., Alexandria Engineering Journal, 59 (2020) 177-189.
[29] M. Shamshuddin, A. Saeed, S. Mishra, R. Katta and M. R. Eid., International Journal of Numerical Methods for Heat & Fluid Flow, (2023).
[30] P. Sreedevi, and P.S. Reddy, Heat Transfer—Asian Research, 48 (2019) 4105-4132.
[31] A. Tulu and W. Ibrahim, Mathematical Problems in Engineering, 2020 (2020) 1-13.
[32] F. Saba, N. Ahmed, U. Khan and S. T. Mohyud-Din., International Journal of Heat and Mass Transfer, 136 (2019) 186-195.
[33] M. I. Ur Rehman, H. Chen, A. Hamid, W. Jamshed, M. R. Eid, H. A. El-Wahed Khalifa., Numerical Heat Transfer, Part B: Fundamentals, (2023) 1-17.
[34] S. Areekara, A. S. Sabu, A. Mathew and B. Saravanan., Heat Transfer, 50 (2021) 6680-6702.
[35] T.S. Neethu, S. Areekara, and A. Mathew, Heat Transfer, 50 (2021) 5170-5197.
[36] A. Sabu, A. Mathew, T. Neethu and K. A. George., Thermal Science and Engineering Progress, 22 (2021) 100816.
[37] W. Khan and I. Pop, International journal of heat and mass transfer, 53 (2010) 2477-2483.